

# AIAA'86

**AIAA-86-1304**

**The Circulating Balls Heat  
Exchanger (CIBEX)**

N. Gat, TRW Space and Technology  
Group, Redondo Beach, CA

**AIAA/ASME 4th Joint Thermophysics and  
Heat Transfer Conference**

June 2-4, 1986/Boston, Massachusetts

# THE CIRCULATING BALLS HEAT EXCHANGER (CIBEX)

Nahum Gat

TRW, Space and Technology Group

Redondo Beach, CA

## Abstract

The CIBEX heat exchanger consists of a gas cooling section (gas generator) and an air heating section (air preheater) coupled with a stream of solid particles. The stream of particles falls through a hot gas stream, picking up heat and cooling the gas, then through the air stream, heating the latter. The cooled particles are then returned to the top of the device and the heating/cooling cycle repeated. The paper describes the two-phase equations of motion for the flow of the spherical particles through the fluid. The solid phase is treated as a pseudo-gas by using concentrations instead of density. The equations are then non-dimensionalized and solved by numerical integration. The solution gives temperature and velocity profiles for the two phases for parametric variations in the solid loading and the fluid flux rate. The solution is applied for the design of a heat exchanger for a hypothetical 2500 tons/day coal gasification plant. The dimensions of the CIBEX heat exchanger are much smaller than those of a comparable conventional heat exchanger.

## Nomenclature

A	Flow cross section area
A, B, C, D, E, F	Variables, defined in Table 5
$C_D$	Drag Coefficient
$C_{pg}$	Specific Heat of Gas
$C_{pp}$	Specific Heat of Particle
$d_p$	Particle Diameter
g	Gravitational Acceleration
h	Heat Transfer Coefficient (Combined convective and radiative effects)
H	Enthalpy
$k_g$	Gas Thermal Conductivity
$k_p$	Particle Thermal Conductivity
L	Heat Exchanger Length
$\dot{m}_g$	Gas Flow Rate
$\dot{m}_p$	Particle Flow Rate
$n_p$	Particle Number Density
P	Pressure
$Q_w$	Heat Loss to Wall
R	Gas Constant
T	Temperature
U	Velocity

## Greek Letters

$\gamma$	Specific Heat Ratio for Gas
$\epsilon$	Volume Fraction of Solids
$\eta$	Loading Factor
$\mu$	Viscosity
$\rho$	Density
$\phi$	Concentration
$\xi$	Dissipation Tensor

## Subscripts

g	Gas
i	Inlet
p	Particle
w	Wall
0	at $x=0$ bottom of heat exchanger
1	at $x=1$ top of heat exchanger

## Superscripts

*	Dimensional Quantity
$\vec{\phantom{x}}$	Vector Quantity
( )	Derivative with respect to x

## Introduction

The paper describes a concept of a direct contact heat exchanger/regenerator in which one medium (gas) flows through a moving bed of a second medium (solid particles) and exchanges heat with it. The concept may be utilized for regenerative heat transfer between the high temperature combustion gas stream and the cold combustion air of, for instance, a combustor for a MHD generator<sup>1</sup>, or for enhancing chemical reactions between a flowing gas stream and a solid material in the metallurgical, chemical or petroleum

industries<sup>2,3</sup>. Schematically shown in Figure 1, the solid particles fall through a counter flowing hot gas stream in the gas generator. The gas cools down by heat transfer to the particles. The particles then fall through the air preheater in which they give off heat to the combustion air. The particles are then recirculated back into the gas generator via a pneumatic or mechanical lift. The concept is of interest because of its high potential to provide relatively maintenance free heat exchange in a compact package and is particularly suitable for a stream of dirty combustion products such as in coal combustors and gasifiers. In addition such a heat exchanger is smaller in size than similarly rated conventional heat exchangers, it provides greater heat recovery, low pressure drop and easy access for cleaning.

## 1. Mathematical Formulation

The two phase counter flow in the heat exchanger can be described by writing the conservation equations (mass, momentum and energy) for each phase separately, including the terms for

interaction between the phases<sup>4</sup>. In theory, the gas flows in the open spaces between the particles. As the number density of the

particles changes, so does the available cross-section area for the gas flow. To avoid the issue of dealing with a variable area flow, the problem is formulated in terms of concentrations rather than densities. Several definitions, listed in Table 1, are helpful. With these definitions, the stream of particles is treated here as a pseudo-gas, or a continuum, having a "density" specified by its concentration. The following is a list of assumptions underlying the analysis.

1. Steady 1-D flow.
2. Particles are uniformly distributed over each cross section.
3. Particles are spherical and of a uniform size.
4. The volume occupied by the particles cannot be neglected.
5. Particles are spread far enough so that the motion of each one is unaffected by the motion of its neighbors or by the wake of the preceding particles.
6. The particles are large enough and no random motion (Brownian type motion) exists. The pressure in the mixture is that of the gas.
7. Particles do not interact with the boundaries and in the case of uniform size distribution, particles do not interact with each other.
8. The boundary layer effect on the flow is neglected.
9. Gas is perfect, compressible and its physical properties are a function of temperature only.
10. The temperature of each particle is uniform with no internal gradients.

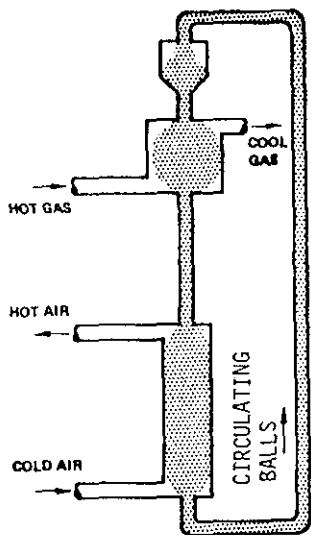


Figure 1. The CIBEX concept

Table 1: Basic Definitions of two phase flow quantities

Quantity	Definition	Units
Number density of particles	$n_p^* = \frac{\dot{m}_p^* / A^*}{\rho_p^* \frac{\pi d_p^{*3}}{6} U_p^*}$	Particles/Volume
Volume fraction occupied by the particles	$\epsilon = n_p^* \frac{\pi d_p^{*3}}{6}$	Dimensionless
Volume fraction occupied by the gas	$1 - \epsilon$	Dimensionless
Gas concentration	$\sigma_g^* = \rho_g^* (1 - \epsilon)$	Weight/volume
Particles Concentration	$\sigma_p^* = \rho_p^* \epsilon$	Weight/volume
The loading ratio	$\eta = \frac{\dot{m}_p^*}{\dot{m}_g^*} = \frac{\sigma_p^* U_p^*}{\sigma_g^* U_g^*}$	Dimensionless

Equations of Motion

The equations of motion are listed in Table 2 for the gas and solid phases. In equation (3), the change in momentum is attributed to the body forces acting upon the pseudo-gas phase. The second term on the right hand side is the drag force per unit volume. In equation (5), it is assumed that the change in the energy of the particles occurs solely due to heat exchange with the environment. The heat transfer coefficient,  $h^*$ , may be composed of both a convective and a radiative terms. Presently only the convective term is taken into account.

In equation (6),  $Q_w^*$  is the rate of heat loss to the walls

$$\dot{Q}_w^* = \rho_{gi}^* C_{pgi}^* T_g^* \frac{U_{gi}^*}{L^*} \alpha$$

and  $\alpha$  designates the fraction loss. Other terms in the gas energy equation stand for the pressure work, thermal conductivity, viscous dissipation and heat exchange with the particles.

The Equation of State: It can be shown that the pressure in the system is composed of the partial pressures of the two phases. For a mixture in thermal equilibrium,

$$p^* = \sigma_m^* R^* T^*$$

where

$$\sigma_m^* = \sigma_g^* + \sigma_p^* = (1 - \epsilon) \rho_g^* + \epsilon \rho_p^*$$

Thus, for a mixture in which the partial volume of solids is small ( $\epsilon \ll 1$ ) the partial pressure of the solids may be neglected and the equation of state for the gas and solid phases are given on Table 2.

Table 2a: Equation of motion for the two phase flow

<u>SOLID PHASE</u>	
<u>Continuity</u>	
$\sigma_p^* u_p^* A^* = \dot{m}_p^*$	(1)
<u>Momentum</u>	
$\sigma_p^* \frac{DU_p^*}{Dt^*} = \sigma_p^* \vec{g}^* - \frac{\sigma_g^*}{2} \left( \frac{\vec{U}_p^* - \vec{U}_g^*}{ \vec{U}_p^* - \vec{U}_g^* } \right) \left( U_p^* - U_g^* \right) C_D A_p^* n_p^*$	(3)
<u>Energy</u>	
$\sigma_p^* \frac{DH_p^*}{Dt^*} = -h^* A_s^* n_p^* (T_p^* - T_g^*)$	(5)
<u>State</u>	
$\rho_p^* = \text{constant}$	(7)
<u>Transport Properties</u>	
$C_{pp}^* = \text{constant}$	(9)

Table 2b: Equation of motion for the two phase flow

<u>GAS PHASE</u>	
<u>Continuity</u>	
$\sigma_g^* u_g^* A^* = \dot{m}_g^*$	(2)
<u>Momentum</u>	
$\sigma_g^* \frac{DU_g^*}{Dt^*} = -\nu \rho^* + \nu \cdot \vec{\tau} + \frac{\sigma_g^*}{2} \left( \frac{\vec{U}_p^* - \vec{U}_g^*}{ \vec{U}_p^* - \vec{U}_g^* } \right) \left( U_p^* - U_g^* \right) C_D A_p^* n_p^*$	(4)
<u>Energy</u>	
$\sigma_g^* \frac{DH_g^*}{Dt^*} = U_g^* \frac{dp^*}{dx^*} + h^* A_s^* n_p^* (T_p^* - T_g^*) + \dot{Q}_w^* + k_g^* \frac{d^2 T_g^*}{dx^{*2}} + \frac{4}{3} \mu^* \left( \frac{dU_g^*}{dx^*} \right)^2$	(6)
<u>State</u>	
$p^* = \sigma_g^* R^* T_g^*$	(8)
<u>Transport Properties</u>	
$\frac{C_{pg}^*}{R^*} = 4.7692 - \frac{970.85}{T_g^*} + \frac{1.803 \times 10^{-5}}{T_g^{*2}}$	(10)
$\mu_g^* = 1.78 \times 10^{-5} \left( \frac{T_g^*}{300} \right)^{0.5} \left[ \frac{\text{Kg}}{\text{m sec}} \right]$	(11)
$k_g^* = 4.982 \times 10^{-2} + 5.164 \times 10^{-5} (T_g^* - 700) \left[ \frac{\text{W}}{\text{m K}} \right]$	(12)

Transport Properties: For simplicity it is assumed that the specific heat of the solid phase is constant. For the gas the dependence of the transport properties on the temperature is given in Table 2.

In summary, the number of unknowns is seven ( $\rho_g^*, T_g^*, p_g^*, T_p^*, U_g^*, U_p^*, \epsilon$ ), same as the number of equations (1, 2, 3, 4, 5, 6, and 8).

Coordinate System: The positive x direction is chosen in the upwards direction, and the velocity vector can be expressed in terms of the scalar speed as  $\vec{U}_p = U_p \vec{x}$ , and  $\vec{U}_g = U_g \vec{x}$ . Similarly the

following relationships are useful  $dx_p = U_p dt$ ,  $dx_g = U_g dt$ , and  $\vec{g} = -g \vec{x}$ .

Nondimensional equations: The following terms are used to nondimensionalize the equations:

$$x = \frac{x^*}{L^*}, \quad \sigma = \frac{\sigma^*}{\rho_g^*}, \quad U = \frac{U^*}{U_{gi}^*}, \quad T = \frac{T^*}{T_{gi}^*},$$

$$\mu_g = \frac{\mu_g^*}{\mu_{gi}^*}, \quad k_g = \frac{k_g^*}{k_{gi}^*}, \quad C_{pg} = \frac{C_{pg}^*}{C_{pgi}^*}$$

Next, to reduce the number of equations and variables, the two continuity equations are substituted into the corresponding momentum and energy equations. Similarly, the equation of state is substituted into the momentum and energy equations. Using the coordinate system and the dimensionless parameters, and after some rearrangement, the four equations with four unknowns  $T_g, U_g, T_p$  and  $U_p$  can be written as

shown in Table 3. The table also gives the definition of the dimensionless numbers appearing in the problem. Finally, the drag coefficient, heat transfer coefficient, and additional quantities which are calculated at the local conditions are given in Table 4.

Table 3: Reduced equations of motion and the dimensionless quantities

Momentum	$\frac{dU_p}{dx} = -\frac{1}{U_p Fr} + \frac{3}{4} \frac{(U_p + U_g)^2}{U_p U_g} \frac{C_D}{S} \quad (13)$
	$\frac{dU_g}{dx} = -\frac{1}{\gamma M_i^2} \frac{d}{dx} \left( \frac{T_g}{U_g} \right) - \frac{3}{4} \frac{(U_p + U_g)^2}{U_p U_g} \frac{C_D}{S} - \frac{4}{3} \frac{d^2 U_g}{dx^2} \quad (14)$
Energy	$\frac{dT_p}{dx} = 6 \frac{Nu}{Re Pr} k_g C_{pr} \frac{(T_p - T_g)}{S u_p} \quad (15)$
	$\frac{d}{dx} \left[ \left( \frac{C_{pg}^*}{R^*} \right) T_g \right] = U_g \frac{d}{dx} \left[ \frac{T_g}{U_g} \right] + 6 \frac{Nu}{Re Pr} k_g \left( \frac{C_{pgi}^*}{R^*} \right) \frac{(T_p - T_g)}{S u_p} + \left( \frac{C_{pgi}^*}{R^*} \right) \frac{d^2 T_g}{dx^2} + \frac{\gamma M_i^2}{Re(L/d)} \left( \frac{dT_g}{dx} \right)^2 - \left( \frac{C_{pg}^*}{R^*} \right) T_g \alpha \quad (16)$
Dimensionless Reference Quantities	Reynolds number $Re = \frac{u_{gi}^* U_{gi}^* d_p^*}{\mu_{gi}^*} = \frac{m^*/A^* d_p^*}{\mu_{gi}^*} \quad (-) \quad S = \left( \frac{d_p^*}{L^*} \right) \left( \frac{\rho_p^*}{\rho_{gi}^*} \right)$
	$Re_p = Re \frac{U_p/U_g + 1}{u_g}$
	Prandtl number $Pr = \frac{u_{gi}^* C_{pgi}^*}{k_{gi}^*}$ Mach number $M_i = \frac{U_{gi}^{*2}}{\gamma R^* T_{gi}^*}$
	Peclet number $Pe = Re Pr$ Nusselt number $Nu = h^* \frac{d_p^*}{k_g^*}$
	Froude number $Fr = \frac{U_{gi}^{*2}}{L^* g^*}$ Stanton number $St = \frac{Nu}{Re Pr} = \frac{Nu}{Pe}$

Table 4: Drag and heat transfer coefficients

<u>Drag coefficient</u>	
$C_D = \frac{24}{Re_p} + 4.5$	for $0 < Re_p < 1$
$\lg C_D = \lg 28.5 - \frac{24}{28.5} \lg Re_p + 0.06919 (\lg Re_p)^2$	for $1 \leq Re < 60$
$\lg C_D = 2.0065 - 1.3830 \lg Re_p + 0.19887 (\lg Re_p)^2$	for $60 \leq Re < 300$
$C_D = 0.4$	for $C_D \geq 3000$
<u>Heat transfer coefficient</u>	<u>Local Viscosity</u>
$Nu = 2 + 0.6 Re_p^{1/2} Pr_p^{1/3}$	$\mu_g = T_g^{1/2}$
<u>Local Prandtl number</u>	<u>Ratio of specific heats between gas and particles</u>
$Pr_p = Pr \frac{\mu_g C_{pg}}{k_g}$	$C_{pr} = C_{pgi}^*/C_{ppi}^*$

Boundary Conditions: The boundary conditions are specified for the gas at the bottom (i.e., at  $x = 0$ ) and for the particles at the top ( $x = 1$ ) of the heat exchanger. The nondimensional boundary conditions are therefore,

$$\begin{aligned} \text{at } x = 0, T_g = 1 \quad \text{and} \quad U_g = 1 \\ \text{at } x = 1, T_p = T_{p1} \quad \text{and} \quad U_p = 0 \end{aligned} \quad (17)$$

Here  $T_{p1} = T_{p1}^*/T_g^*$  is the inlet temperature of the solid phase.

Solution: An order of magnitude analysis indicates that the Reynolds number may vary from 5 to 2500. The heat exchanger dimension,  $L^*/d_p^*$ , is of the order of 1,000 to 10,000. The quantity  $S$  is between 1 to 50, and the Mach number is smaller than 0.001. Accordingly, only meaningful terms are kept in the equations of motion. The second derivative of velocity term is dropped (Eq. 14), the thermal conductivity term and the dissipation term in Equation 16 are dropped, but the pressure work terms are retained (Eqs. 14 and 16). By further differentiation and rearrangement, Equations 13 to 16 may be expressed as four equations with four unknowns which are the following derivatives:  $U_p'$ ,  $U_g'$ ,  $T_p'$ ,  $T_g'$

Table 5: The reduced equation of motion

$$\begin{aligned} U_p' + 0 + 0 + 0 &= -\frac{1}{U_g Fr} + A \frac{C_D}{S} & (18) \\ 0 + B U_g' + C T_g' + 0 &= -A \frac{C_D}{S} n & (19) \\ 0 + 0 + 0 + T_p' &= 6 S_t k_g C_{pr} \frac{D}{S} & (20) \\ 0 + F U_g' + E T_g' + 0 &= 6 S_t k_g \left(\frac{C^* p g i}{R^*}\right) \frac{D}{S} n - Q & (21) \end{aligned}$$

where

$$\begin{aligned} A &= \frac{3}{4} \frac{(U_p + U_g)^2}{U_p U_g} & D &= \frac{T_p - T_g}{U_p} \\ B &= 1 - \frac{T_g}{\gamma M_i^2 U_g^2} & E &= 3.7692 - \frac{1.803 \times 10^5}{T_g^2} \\ C &= \frac{1}{\gamma M_i^2 U_g} & F &= \frac{T_g}{U_g} \\ & & Q &= \alpha \frac{C^* p g i}{R^*} T_g \end{aligned}$$

Table 6: The equations of motion in a convenient form for numerical integration

$$\begin{aligned} U_p' &= -\frac{1}{U_g Fr} + A \frac{C_D}{S} & (22) \\ U_g' &= \left[ \left( 6 S_t k_g \left(\frac{C^* p g i}{R^*}\right) \frac{D}{S} n - Q \right) C + A n \frac{C_D}{S} E \right] / \Delta & (23) \\ T_g' &= \left[ -A n \frac{C_D}{S} F - \left( 6 S_t \frac{D}{S} k_g \left(\frac{C^* p g i}{R^*}\right) n - Q \right) B \right] / \Delta & (24) \\ T_p' &= 6 S_t C_{pr} D \frac{k_g}{S} & (25) \end{aligned}$$

Where

$$\Delta = CF - BE \quad (26)$$

(the prime denotes the derivative with respect to the  $x$  coordinate) as shown in Table 5. Finally, to facilitate numerical integration, equations 18 to 21 can be solved, and the four unknowns expressed in terms of the independent variables as shown in Table 6. This formulation is particularly convenient for use in numerical integration once the boundary conditions are specified.

## 2. Results

The set of equations (22) to (25) has been solved numerically, using boundary conditions (17). The integration follows the Runge-Kutta technique and it requires a guess of the solution at  $x=1$  so that the integration may proceed from  $x=1$  down to  $x=0$ . If the derived conditions at the bottom ( $x=0$ ) do not match the given B.C.s, a new guess is made and the integration is repeated. An intelligent new guess can be made on the basis of the results of the integration. This "shooting" technique is repeated until all B.C.s are matched.

In order to obtain a realistic solution to the problem, the heat exchanger has been matched with a hypothetical coal gasification plant. A block diagram of the complete plant is shown in Figure 2. The heat exchanger model is solved then to select the optimal dimensions of the gas generator, the air preheater, and the balls' material and size. The parameters variation included the following:

- pressure: 6 and 30 atm.
- balls material: stainless steel (density 8330 kg/m<sup>3</sup>,  $C_p = 461$  J/kgK) and ceramic (density 3717 kg/m<sup>3</sup>,  $C_p = 1047$  J/Kg K)
- balls size 1, 1.6, 2.0 mm
- loading parameter from 0.8 to 2.0

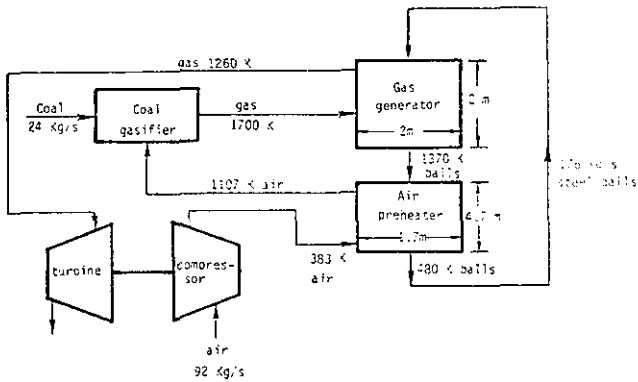


Figure 2. Approximate sizing of a 2500 ton/day coal gasification plant operating at 30 atm and utilizing a CIBEX.

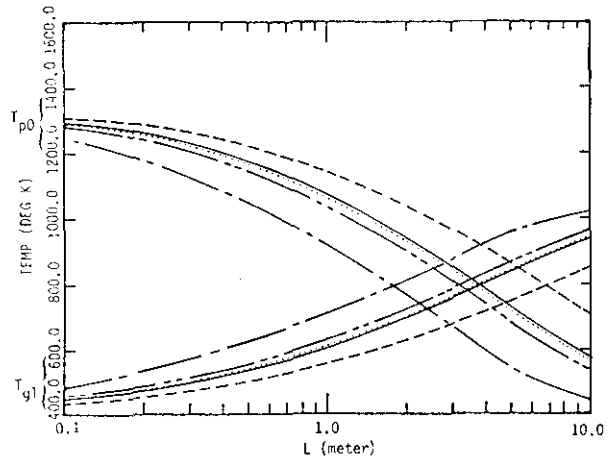


Figure 4.  $T_{g1}$  and  $T_{p0}$  variation with length of air preheater,  $d_p=1.6\text{mm}$ , 6 and 30 atm., stainless steel balls. (legend as in Figure 3)

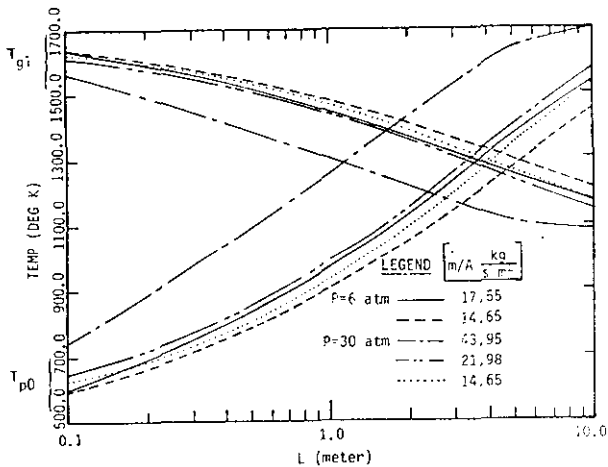


Figure 3.  $T_{g1}$  and  $T_{p0}$  variation with length of gas generator,  $d_p=1.6\text{mm}$ , Pressure is 6 and 30 atm., stainless steel balls.

Typical results of these calculations are shown in Figures 3 through 8. These results have been used for the sizing of the heat exchanger unit in Figure 2. Figure 3 shows the heat exchange between the gas and stainless steel balls in the gas generator. The figure shows the balls' temperature at the bottom of the gas generator, and the gas temperature at the top of the generator for different lengths of generator. Similarly, Figure 4 shows the balls temperature at the bottom, and the air temperature at the top of the air preheater. In both figures, the parameters are the operating pressure and the air/gas flow rate. The maximum air/gas flow rate is limited by the terminal velocity of the balls. At a too high velocity the balls are blown out of the unit. The velocity of the balls and of the gas in the gas generator and in the air preheater is shown in Figures 5 and 7. The balls initial velocity (at the top) is always zero and they reach their terminal velocity in a short distance. The terminal velocity changes however along the way, because of variations in

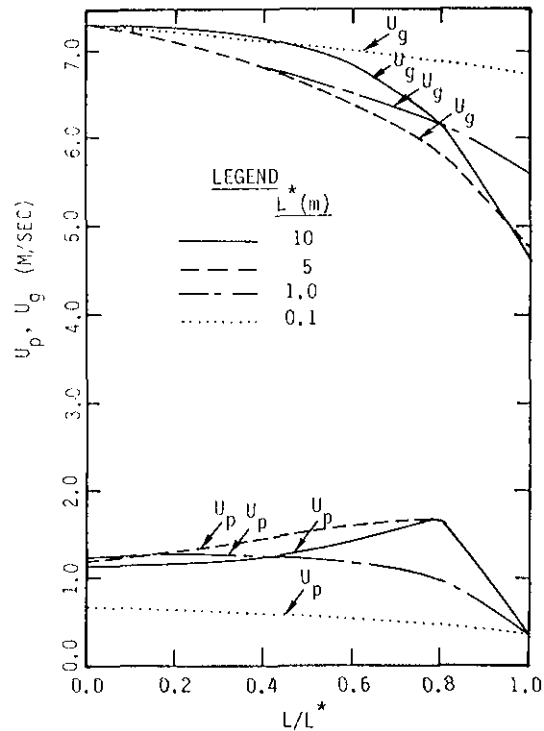


Figure 5. Gas velocity and particle velocity in gas generator, stainless steel balls,  $d_p=1.6\text{mm}$ ,  $P=30\text{ atm.}$ ,  $\dot{m}_p/A=43.95\text{ Kg/m}^2\text{ sec.}$

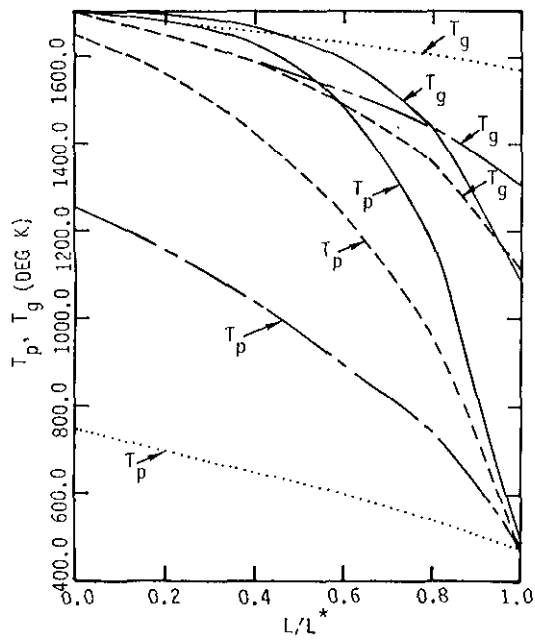


Figure 6. Gas temperature and particle temperature in gas generator, stainless steel balls,  $d = 1.6\text{mm}$ ,  $P = 30$  atm.,  $\dot{m}/A = 43.95 \text{ Kg/m}^2 \text{ sec}$ . (legend as in Figure 5)

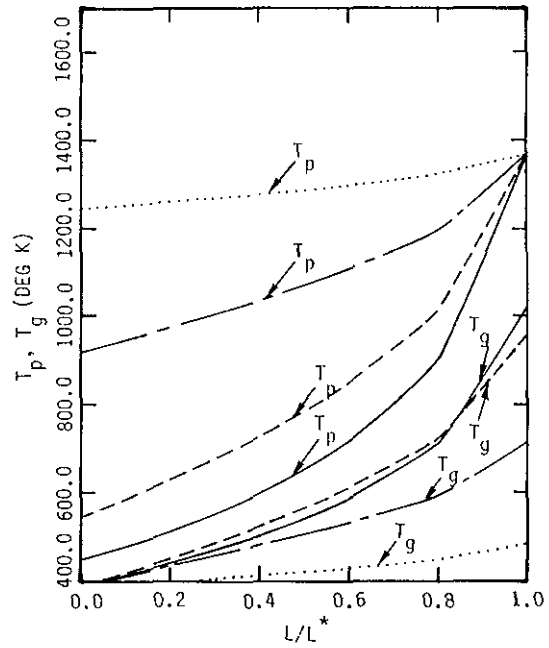


Figure 8. Gas temperature and particle temperature in air preheater, stainless steel balls,  $d = 1.6\text{mm}$ ,  $P = 30$  atm.,  $\dot{m}/A = 53.43 \text{ Kg/m}^2 \text{ sec}$ . (legend as in Figure 5)

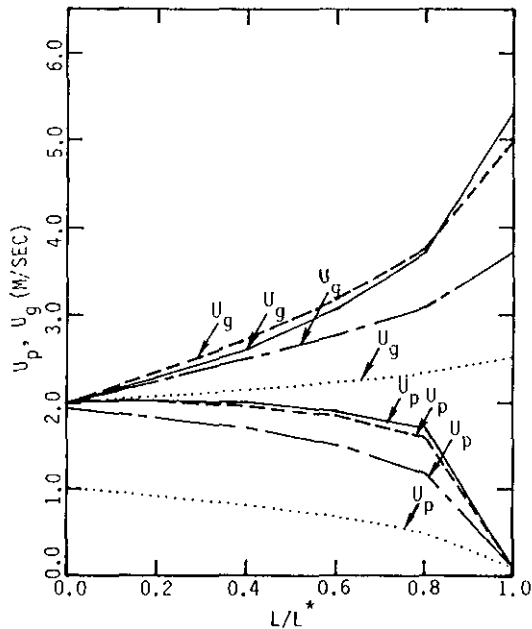


Figure 7. Gas velocity and particle velocity in air preheater, stainless steel balls,  $d = 1.6\text{mm}$ ,  $P = 30$  atm.,  $\dot{m}/A = 53.43 \text{ Kg/m}^2 \text{ sec}$ . (legend in Figure 5)

gas temperature. The gas and ball temperature variations is shown in Figures 6 and 8 for the gas generator and air preheater, respectively. Based on these calculations the heat exchanger in Figure 2 was sized to meet the plant requirements.

### 3. Conclusions

- o A heat exchanger based on the CIBEX concept is smaller in size than a comparably rated conventional heat exchanger.
- o The computer code can be exercised to size and to design both units of the heat exchanger; the gas generator and the air preheater. Some features that the code indicates are:
  - Small balls are preferable to large ones since they have a larger surface area per unit weight and they have a longer residence time (smaller terminal velocity). But too small balls limit the mass flux and therefore an optimal ball size exists for each application.
  - Increased operating pressure reduces the overall size of the heat exchanger.



### References

On a unit mass basis ceramic balls are more effective than stainless steel balls. However, durability of ceramic may not be as good as that of the stainless balls.

- o The CIBEX concept is uniquely capable of recovering very high level heat from effluent gases which may contain very reactive gas species such as  $H_2S$ ,  $CO_2$ ,  $CO$ , etc. In this case ceramic balls are the preferred heat transfer material.

### Acknowledgement

The author wishes to thank the following individuals at TRW who sponsored and guided the work: A. P. Grossman, L. Manson, H. Burge.

1. Heywood, and Womack. "Open Cycle MHD Power Generation." Pergamon Press, 1969, 194-212.
2. "Method for Effecting Chemical Reactions Between Cascading Solids and Counterflowing Gases or Fluids." U. S. Patent 3,801,469, April 1974.
3. Yoon, S. M., and Kunii, D., "Gas Flow and Pressure Drop Through Moving Beds." Ind. Eng. Chem. Process Des. Develop., Vol. 9, No. 4, 1970. 559-565.
4. Marble, F. E. "Dynamics of Dusty Gases." Annual Review of Fluid Mechanics, Vol. 2, 1970.